Statistical study of high energy radiation from rotation-powered pulsars

ZHENG Guangsheng (CHENG Kwongsang, 郑广生)[1]
& ZHANG Li (张 力)[1,2]

1. Department of Physics, University of Hong Kong, Pokfulam Road, Hong Kong, China;
2. Department of Physics, Yunnan University, Kunming 650091, China
Correspondence should be addressed to Zheng Guangsheng.

Received December 7, 1998

Abstract Based on our self-consistent outer gap model for high energy emission from the rotation-powered pulsars, we study the statistical properties of X-ray and γ-ray emission from the rotation-powered pulsars, and other statistical properties (e.g. diffuse γ-ray background and unidentified γ-ray point sources) related to γ-ray pulsars in our Galaxy and nearby galaxies are also considered.

Keywords: **gamma rays, theory-pulsars, general-stars, neutron-stars, statistics.**

Observationally, the upper limits on pulsed γ-ray emissions for 350 of 706 radio pulsars have been obtained by EGRET. Of these pulsars, only six have been confirmed to emit high energy γ-rays in the energy range of EGRET. Furthermore, 96 unidentified Galactic γ-ray point sources (where 30 unidentified point sources are in low galactic latitudes $|b| < 5°$) have been found. Furthermore, ROSAT and ASCA satellites have detected 33 X-ray pulsars which are also radio pulsars. These observed data allow us to perform useful statistical studies of the observed X-ray/γ-ray pulsar parameters such as the distance, period, age, magnetic field and γ-ray flux distributions, which may provide clues about how to predict possible candidates for X-ray/γ-ray pulsars and can also be used to test the validity of the various γ-ray pulsar models.

Generally, the pulsar models which describe high energy emission from the pulsars can be divided into polar gap models (e.g. refs. [1,2]) and outer gap models[3—10]. Based on various models for γ-ray production from pulsars, many authors have studied detailed statistical properties of γ-ray pulsars by using Monte Carlo methods[11—13]. Here, we will use our model proposed by Zhang and Cheng[10] to determine general formulae for the flux, the luminosity and conversion efficiency of X-rays/γ-rays from the pulsars, and present the statistical analysis of X-ray/γ-ray pulsars.

1 X-ray and γ-ray emission

1.1 The self-sustained outer gap

We have proposed a self-consistent model of the outer gap to describe the high energy γ-ray pulsar emission of the pulsars. In our model the characteristic photon energy $E_\gamma(f)$ is completely determined by the size of the outer gap (f). Half of the primary $e^\pm$ pairs in the outer gap will move toward the star and loss their energy via the curvature radiation. The return particle flux can

be approximated by $\dot{N}_{e^\pm} \approx \frac{1}{2} f \dot{N}_{GJ}$, where f is the fractional size of the outer gap and $\dot{N}_{GJ}$ is the Goldreich-Julian particle flux. Although most of the energy of the primary particles will loss on the way to the star via curvature radiation, about $10.6P^{1/3}$ erg per particle will still remain and finally deposit on the stellar surface. This energy will be emitted in term of X-rays from the stellar surface. The characteristic energy of X-rays is given by $E_X^h \approx 3kT \approx 1.2 \times 10^3 P^{-1/6} B_{12}^{1/4}$ eV, where P is pulsar period in unit of second, B_{12} is the dipolar magnetic field in units of 10^{12} G and the radius of the neutron star is assumed to be 10^6 cm. However the keV X-rays from a hot polar cap will be reflected back to the star due to the cyclotron resonance scattering if there is large density of magnetic produced $e^\pm$ pairs near the neutron star surface, and eventually re-emit soft thermal X-rays with characteristic energy $E_X^s \approx 0.1 f^{1/4} P^{-1/4} E_X^h$. Despite the X-ray photon density is very low, every pair produced by X-ray and curvature photons collision can emit 10^5 photons in the gap. Such huge multiplicity can produce sufficient number of $e^\pm$ pairs to sustain the gap as long as the center of mass energy of X-ray and curvature photon is higher than the threshold energy of the electron/positron pair production, i.e. $E_X E_\gamma \geqslant (m_e c^2)^2$. From the condition for the photon-photon pair production, the fractional size of the outer gap limited by the soft thermal X-rays from the neutron star surface can be determined as

$$f = 5.5 P^{26/21} B_{12}^{-4/7}. \tag{1}$$

It should be emphasized that $f \leqslant 1$. Any fluctuation of the gap can be stabilized by the process described above. In fact, the increase of gap size will increase the X-ray flux and the over-produced pairs can reduce the gap size. Similarly, the decrease of the gap size will produce insufficient pairs and results in the increase of the gap size.

1.2 X-ray emission from pulsar magnetosphere

X-ray emission from a rotation-powered pulsar has been modeled by multi-component X-ray emission. Generally, it consists of two hard thermal components, one soft thermal component and one non-thermal component. For the thermal X-rays, the first hard thermal X-ray component results from polar cap heating by the return current in the polar gap. The second one with a typical energy $E_X^h \approx 1.2 \times 10^3 P^{-1/6} B_{12}^{1/4}$ eV results from polar cap heating by the return particles from the outer gap. Because of cyclotron resonance scattering, most of the hard thermal X-rays will be effectively reflected back to the stellar surface and eventually reemitted as soft thermal X-rays with a typical energy $(E_X^s/E_X^h) \approx 0.1 f^{1/4} P^{-1/4}$. However, some of the hard thermal X-rays can still escape along the open magnetic field lines, where the e^+/e^- pairs density is low. The non-thermal X-rays come from synchrotron radiation of $e^\pm$ pairs created in the strong magnetic field near the neutron star surface by curvature photons emitted by charged particles on their way from the outer gap to the neutron star surface. An electromagnetic cascade will take place until the energy of synchrotron photons is ~ 1 MeV and the spectral index ~ -2 (see refs. [14, 15] for details).

The total number of secondary $e^\pm$ pairs created in the electromagnetic cascade is given by $\dot{N}^{(2)} = (\dot{N}^{(1)} \gamma mc^2/E_0)(r_s/fr_i)^2$ s^{-1}, where $\dot{N}^{(1)} \approx f\dot{N}_{GJ}$ and $\dot{N}_{GJ} = 2.7 \times 10^{30} B_{12} P^{-2}$ s^{-1} is the Goldreich-Julian particle flux, $E_0 \approx 1$ MeV, $r_i \sim 4R_L/9 \tan^2 \chi$ is the distance to the inner boundary of the outer gap, R_L is the radius of the light cylinder, χ is the magnetic inclination an-

gle and r_s is the distance to the star where the magnetic pairs are produced. Since most of the energy of secondary $e^{\pm}$ is radiated away in form of synchrotron X-rays, we have the X-ray luminosity $L_X \approx E_0 \cdot \dot{N}^{(2)}$. Thus writing $r_s/r_i = (9/4)\tan^2\chi(r_s/R_L)$ and using $\dot{N}^{(2)}$, we obtain

$$L_X \approx 5.5 \times 10^{-4}\left(\frac{\tan\chi}{\tan 55^\circ}\right)^4 B_{12}^{0.13} P_{-1}^{-0.80} L_{sd} \tag{2}$$

and $L_X \approx 10^{-3} L_{sd}$ for the Crab pulsar, where P_{-1} is the pulsar period in units of 0.1 s and L_{sd} is the spin down power of the pulsar. In the case of millisecond pulsars, for which the light-cylinder is much closer to the star than that in canonical pulsars we have to use $r_s \approx R$ (the much stronger multipole surface magnetic field will allow the copious pair production there) and

$$L_X^{msec} \sim 10^{-3}\left(\frac{\tan\chi}{\tan 55^\circ}\right)^4 B_9^{1/12} P_{-2}^{-7/9} L_{sd}. \tag{3}$$

For $P = 0.004$ s, $B_{12} = 0.0005$ and $\chi = 55^\circ$ one obtains $L_X^{msec} = 0.002 \cdot L_{sd}$. The results of calculations corresponding to $\chi = 55^\circ$ in eqs. (2) and (3) for 25 pulsars from table 1 in ref. [16] are presented in ref. [14]. Furthermore, the expected X-ray spectrum for $E_X < 1$ MeV, which consists of thermal X-rays and hard non-thermal X-rays, is given by

$$\frac{d\dot{N}_x}{dE_X} = F_{bb}(T_i, E_X) + AE_X^{-2}, \tag{4}$$

where F_{bb} is the sum of blackbody spectra with characteristic temperatures T_i (subscript i represents soft and two hard thermal X-rays respectively) and A is the normalized coefficient[15]. It should be pointed out that the characteristic blackbody temperatures of the two hard X-ray components, emitted from the polar cap area inside the polar gap and the polar cap area defined by the foot-prints of the outer gap magnetic field lines, are strongly affected by the surface magnetic field, which can be much larger than the dipolar field. In fact, the strong surface magnetic field can explain why the effective blackbody radiation area is nearly two orders of magnitude larger (less) than that deduced from the dipolar field for young (old) pulsars. Our model indicates how several possible X-ray components may be observed depending on the magnetic inclination angle and viewing angle.

1.3 γ-ray emission from pulsar magnetosphere

In our model, γ-rays are produced inside the thick outer gap through synchro-curvature radiation[17] of the primary $e^{\pm}$ pairs. The γ-ray luminosities can be expressed as[10]

$$L_\gamma \approx 3.6 \times 10^{31} f^3 B_{12}^2 P^{-4} \text{ erg} \cdot \text{s}^{-1}. \tag{5}$$

The radiation spectrum produced by the primary particles with power-law distribution in the outer gap can be expressed as[10]

$$\frac{d^2 N_\gamma}{dE_\gamma dt} \approx \frac{\dot{N}_0}{E_\gamma}\int_{x_{min}}^{x_{max}} x^{3/2}\frac{R_L}{r_c}\left[\left(1+\frac{1}{r_c^2 Q_2^2}\right)F(y) - \left(1-\frac{1}{r_c^2 Q_2^2}\right)yK_{2/3}\right]dx, \tag{6}$$

where $\dot{N}_0 = \sqrt{3}\, e^2 \gamma_0 N_0 / hR_L$, $N_0 \approx 1.4 \times 10^{30} f(B_{12}/P)$ and $\gamma_0 \approx 2 \times 10^7 f^{1/2}(B_{12}/P)^{1/4}$, $r_c = xR_L/[(1 + r_B/(xR_L))\cos^2\alpha + (R_L/r_B)x\sin^2\alpha]$, and $Q_2 = (1/xR_L)[((r_B/xR_L) + 1 - 3(R_L/r_B)x)\cos^4\alpha + 3(R_L/r_B)x\cos^2\alpha + (R_L/r_B)^2 x^2 \sin^4\alpha]^{1/2}$; x_{min} and x_{max} are minimum and maximum curvature radii of the magnetic field lines in units of radius of light cylinder; $r_B = \gamma mc^2 \sin\alpha / eB$, α is the pitch angle of charged particle in the curved magnetic field (B) and α

$\approx 0.79\, f^{1/2} B_{12}^{-3/4} P^{7/4} x^{17/4}$; $F(y) = \int_y^\infty K_{5/3}(z)\mathrm{d}z$, where $K_{5/3}$ and $K_{2/3}$ are the modified Bessel functions of order 5/3 and 2/3, and $y = E_\gamma / E_c$. The characteristic energy of the radiated photons is given by $E_c \approx 640.5\ (P/B_{12})^{3/28} x^{-13/4} (R_L x Q_2)$ MeV. Therefore, the differential flux at the earth is given by

$$F(E_\gamma) = \frac{1}{\Delta\Omega d^2} \frac{\mathrm{d}^2 N_\gamma}{\mathrm{d}E_\gamma \mathrm{d}t}, \tag{7}$$

where $\Delta\Omega$ is the solid angle of γ-ray beaming and d is the distance to the pulsar. In this model, there are three parameters, i.e. $\Delta\Omega$, $x_{\min}$ and $x_{\max}$. These three parameters depend on the detailed structure of the outer gap and the inclination angle of the pulsar. We have calculated the energy spectra from X-rays to γ-rays for the known γ-ray pulsars except for Crab pulsar[10,18]. As an example, fig. 1 is the comparison of model result with the observed data of Geminga.

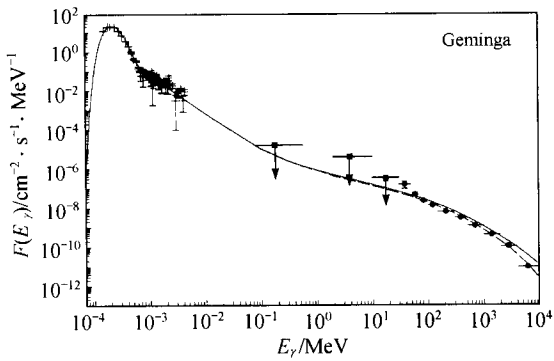

Fig. 1. The spectrum of Geminga. Here $\Delta\Omega = 2.0$, $x_{\min} = 0.7$, $x_{\max} = 2.0$ and $\chi = 55°$ are used.

The expected efficiency of converting spindown power to γ-rays, η_{th}, can be defined by $\eta_{\mathrm{th}} = L_\gamma / L_{\mathrm{sd}}$ where L_γ is total γ-ray luminosity which depends on the model used; L_{sd} is the spindown power and proportional to $p^{-4} B^2$ in the approximation of dipolar magnetic field. Therefore, the conversion efficiency can be expressed in terms of B_{12} and P

$$\eta_{\mathrm{th}} \approx 1.66 \times 10^2 B_{12}^{-12/7} P^{26/7} \approx 10^{-4} \tau^{6/7} P^2, \tag{8}$$

where τ is the characteristic age in unit of year. It should be pointed out that the pulsars with $f \leqslant 1$ are γ-ray pulsars in our model. Therefore, in the database of Nel et al.[19], we selected the pulsars which satisfy $f \leqslant 1$ as a sample. Together with 6 known γ-ray pulsars, our sample consists of 57 pulsars (including 7 millisecond pulsars). Our result is very consistent with the data. In particular, our model explains why the conversion efficiency of millisecond pulsars is so low because of the P^2 dependence[20].

We have considered high energy γ-ray radiations from the radio pulsars associated with some unidentified EGRET γ-ray sources[21]. The calculated conversion efficiencies and energy spectra of the high energy γ-rays from these possible γ-ray pulsars in the outer gap models are compared with the observed results. Of these possible γ-ray pulsars, our results indicate that (i) PSR B1900 + 05 is not a possible γ-ray pulsar; (ii) although the newly discovered young radio pulsar PSR J1105-6107 is a possible γ-ray pulsar, it may not account for high energy γ-ray emission from 2EG J1103-6106; (iii) the high energy γ-rays from 2EG J1801-2312 and 2EG J1857 + 0118 may not be produced completely by radio pulsars PSR B1758-23 and PSR B1853 + 01 respectively; (iv) the counterparts (radio pulsars PSR B1046-58 and PSR B1823-13) of 2EG J1049-5247 and 2EG J1825-1307 are possible γ-ray pulsars; and (v) 2EG J0008-7307 associated with a young supernova remnant CTA 1 may contain a γ-ray pulsar with period $0.16 \geqslant P \geqslant 0.12$ s.

2 The statistical properties of high energy emission from Young pulsars

Based on our model, we will consider the statistical properties of X-ray and γ-ray pulsars respectively. In order to do so, we use the following conventional assumptions for generating the Galactic pulsar population: (i) the pulsars are born at a rate ($\dot{N}_{NS} \sim (1—2)$ per century) at spin periods of $P_0 = 30$ ms; (ii) the initial positions for each pulsar are estimated from the distributions $\rho_z(z) = (1/z_{\exp})\exp(-|z|/z_{\exp})$ and $\rho_R(R) = (a_R/R_{\exp}^2)R\exp(-R/R_{\exp})$, where z is the distance from the Galactic plane, R is the distance from the Galactic center, $z_{\exp} = 75$ pc, $a_R = [1 - e^{-R_{\max}/R_{\exp}}(1 + R_{\max}/R_{\exp})]^{-1}$, $R_{\exp} = 4.5$ kpc and $R_{\max} = 20$ kpc[13,22]; (iii) the initial magnetic fields are distributed as a Gaussian in log B with mean log $B_0 = 12.5$ and dispersion $\sigma_B = 0.3$, we ignore any field decay for these rotation-powered pulsars; (iv) the initial velocity of each pulsar is the vector sum of the circular rotation velocity at the birth location and a random velocity from the supernova explosion[18, 22].

Once the initial properties of a pulsar at birth are given, the pulsar period at time t can be estimated by

$$P(t) = \left[P_0^2 + \left(\frac{16\pi^2 R_{\rm NS}^6 B^2}{3Ic^3}\right) t\right]^{1/2}, \tag{9}$$

where $R_{\rm NS}$ is the neutron star radius and I is the neutron star moment of inertia. Furthermore, the pulsar position at time t is determined by following its motion in the Galactic gravitational potential. Using the equations given by Paczynski[22] for given initial velocity, the orbit integrations are performed by using the 4th order Runge Kutta method with variable time step on the variables R, V_R, z, V_Z and ϕ. Then the longitude, latitude and the distance of the model pulsar can be calculated. In order to generate a sample pulsar which is detectable at radio band, we need to consider radio selection effects and radio beaming effect. In the radio selection effects, the pulsar must satisfy that its radio flux is greater than the radio survey flux threshold and its broadened pulse width is less than the rotation period[13]. The radio beaming fraction can be expressed as $f_r(\omega) = (1 - \cos\omega) + (\pi/2 - \omega)\sin\omega$, where a random distribution of magnetic inclination angles is assumed and ω is the half-angle of the radio emission cone[23]. Here we will use the model of Lyne and Manchester[24] corrected by Biggs[25], i.e. $\omega = 6°.2 \times P^{-1/2}$. Then, following Emmering and Chevalier[23], a sample pulsar with a given period P is chosen in one out of $f_r(P)^{-1}$ cases using the Monte Carlo method.

2.1 The statistic properties of young galactic X-ray pulsars

We study statistical properties of Galactic population of X-ray pulsars with their ages less than 10^6 a using Monte Carlo method. We will use the Monte Carlo simulation code described in Cheng and Zhang[18] to calculate the distributions of distance, period, age, magnetic field and X-ray flux of the Galactic X-rays pulsars with their ages less than 10^6 a. In order to do so, the following changes have been made: the γ-ray detectability is replaced by X-ray detectability (we take 2×10^{-14} erg·cm^{-2}·s^{-1} as the minimum detectable energy flux), and the magnetic inclination angles of the pulsars have been randomly sampled. We perform Monte Carlo simulations of pulsars born during the past one million years. In the observed sample of Galactic X-ray pulsars listed by Becker and Trümper[16], 18 of 21 X-ray pulsars have their ages less than 10^6 a with the

exception of three old pulsars PSR B1929 + 10, PSR B0950 + 08 and PSR B0823 + 26 (their apparent ages are $10^{6.49}$, $10^{7.24}$ and $10^{6.69}$ respectively. It should be pointed out that these old pulsars have no outer gaps because their fractional sizes are greater than 1 in our model). The expected X-ray energy flux is estimated by either our model or the empirical formula given by Becker and Trümper[16]. In our model, the fractional size of the outer gap for each pulsar is estimated by using eq. (1), if a pulsar has $f > 1$, then the pulsar does not have an outer gap and is excluded in our statistical analysis. When the expected X-ray energy flux of the model pulsar is larger than the minimum detectable energy flux, it should be an X-ray pulsar. In fig. 2, the normalized cumulative distributions of distance, period, age, magnetic field and X-ray energy flux of the pulsars with an initial period of 30 ms in both our model (solid curves) and Becker & Trümper model (dashed curves) are shown. For comparison, the corresponding observed distributions for 18 known Galactic X-ray pulsars with their ages less than 10^6 a are also shown. In the energy flux distribution, there are only 14 pulsars with known X-ray luminosities. The Kolmogorov-Smirnov (KS) test indicates that two model results are consistent with the observations. Finally, we would like to estimate the number of possible Galactic X-ray pulsars from our statistical analysis. Using 2.0×10^{-14} erg·s^{-1}·cm^{-2} as the minimum detectable energy flux (the corresponding $L_{sd}/4\pi d^2 \sim 2.0 \times 10^{-11}$ erg·s^{-1}·cm^{-2}) and the radio pulsars with their ages $\leqslant 10^6$ a in the Princeton pulsar archive, Becker & Trümper model predicts 46 X-ray pulsars. From our simulations, however, the ratio of simulated X-ray pulsar numbers in our model to those obtained by using the empirical formula of Becker and Trümper[16] is about 0.6. Therefore, our model predicts that about 28 canonical pulsars with their ages $\leqslant 10^6$ a should be X-rays emitters. It should be pointed out that our model prediction depends on the minimum detectable energy flux of X-rays. For example, if the minimum detectable energy flux is about 5×10^{-15} erg·s^{-1}·cm^{-2}, then our model predicts that there are about 48 canonical pulsars with their ages less than 10^6 a which emit X-rays. In fact, the minimum detectable energy flux of X-rays by ROSAT depends strongly on the observation time. Fainter sources will be detectable with longer explosure time.

2.2 The statistic properties of Galactic γ-ray pulsars

Cheng and Zhang[18] have studied the statistical properties of the γ-ray pulsars. Using $S_{\gamma,\min} = 3.0 \times 10^{-10}$erg·cm^{-2}·s^{-1} as the minimum detectable γ-ray energy flux, they found that our model can explain the statistical properties (distance, period, age, magnetic field and γ-ray energy flux) of γ-ray pulsars when the simulated results are compared with the observed data. They also expected that about 11 high energy γ-ray pulsars can be found out of ~ 100 detected radio pulsars with age less than 10^6 a. They also compared the simulated Geminga-like pulsars with the unidentified EGRET sources in the Galactic plane and found that the fluxes of Geminga-like pulsars at $|b| < 5°$ concentrate mainly in the range from $\sim 3 \times 10^{-7}$ to $\sim 3 \times 10^{-6}$ cm^{-2}·s^{-1}, which is consistent with the observed data of 30 unidentified point sources detected by EGRET at $|b| < 5°$. Finally, Cheng and Zhang[18] estimated that the number of Geminga-like pulsars is $\sim 37\dot{N}_{100}$ in our Galaxy.

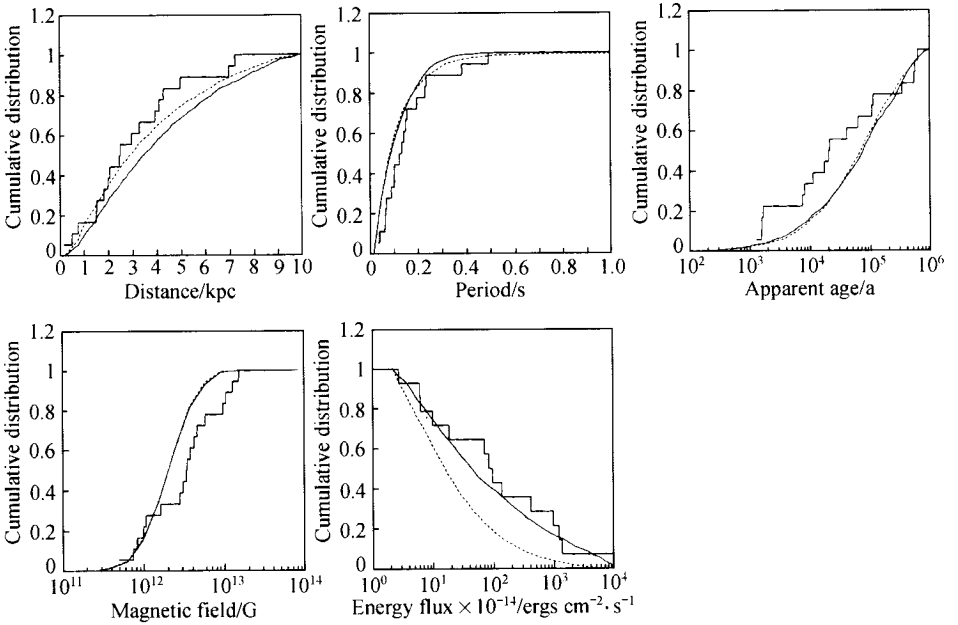

Fig. 2. The normalized cumulative distributions of distance, period, apparent age, magnetic field and energy flux of Galactic X-ray pulsar population with their ages less than 10^6 a for both our model (solid curve) and Becker & Trümper model. For comparison, corresponding distributions of 18 observed X-ray pulsars by ROSAT are also shown (solid histograms).

3 The Galactic diffuse gamma-rays from unresolved rotation-powered pulsars

Recently, EGRET provided more detailed observation of the diffuse γ-ray emission from the Galactic plane. It has been found that the observed intensity exceeds the prediction of cosmic-ray interaction model by as much as 60% above ~ 1 GeV[26]. In order to explain the observed excess, Hunter et al.[26] pointed out two possibilities (also see ref. [27]). The first is that the Galactic cosmic-ray particles have a harder spectrum beyond 10 GeV than those observed in the solar vicinity. However, Mori[28] used the observed cosmic-ray proton flux to calculate the Galactic diffuse γ-ray spectrum and concluded that the observed excess above ~ 1 GeV cannot be explained by revising the models of cosmic-ray interaction with interstellar matter. The second is that the unresolved γ-ray point sources in the Galaxy may contribute their γ-rays to the Galactic diffuse γ-rays. In this section, we consider the second possibility.

The unresolved γ-ray pulsars are those whose γ-ray fluxes are less than the threshold. Using the period, magnetic field strength and distance for each unresolved γ-ray pulsar in our Monte Carlo sample, the diffuse γ-ray differential spectrum from the ith unresolved γ-ray pulsar can be calculated by $F_i(E_\gamma) = (1/\Delta\Omega d_i^2)(d^2N_i/dE_\gamma dt)$, where $d^2N_i/dE_\gamma dt$ is given by eq. (6). The total spectrum which is the superposition of all unresolved γ-ray pulsar's spectra in our Monte Carlo sample is given by $F_{\text{pulsar}}(E_\gamma) = \sum_{i=1}^{n} F_i(E_\gamma)$, where n is the sample number. The spectrum will contribute to the differential spectrum of Galactic diffuse γ-ray.

From our view, the Galactic diffuse γ-rays come mainly from the interaction of cosmic-ray

with interstellar matter and the Galactic unresolved γ-ray pulsars. The total spectrum, F_t, of the Galactic diffuse γ-rays can be expressed as

$$E_t(E_\gamma) = F_{CR}(E_\gamma) + F_{\rm pulsar}(E_\gamma), \quad (10)$$

where $F_{\rm CR}$ is the spectrum produced by the interaction of cosmic rays with the interstellar matter given by Mori[28]. In comparison of model predictions with the observed data, we will use the product of Mori's model prediction in which the cosmic-ray proton spectrum is the median proton spectrum and a parameter $c1$ as the F_{CR}. For the spectrum produced by the unresolved γ-ray pulsars, we only consider the unresolved pulsars in the region of $|b| \leqslant 10°$ and $300° < l < 60°$ and assume that $x_{\rm min} = 0.51$, $x_{\rm max} = 2.1$ and $\Delta\Omega = 2.0$ are the same for all unresolved γ-ray pulsars. Then we calculate the spectrum for a fixed $\dot{N}_{\rm NS100} f_\gamma$.

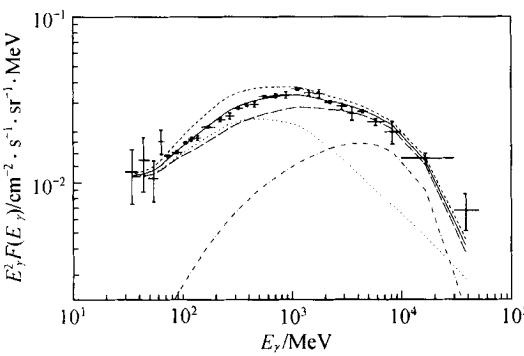

Fig. 3. The diffuse γ-ray differential spectrum, multiplied by E_γ^2, of the Galactic plane. Data are the EGRET observations averaged over $300° < l < 60°$ and $|b| \leqslant 10°$. The model predictions are also shown, which are obtained from eq. (10). The γ-ray spectrum from the unresolved pulsars with $\dot{N}_{\rm NS100} f_\gamma = 1$ has been calculated. The γ-ray spectra produced by the cosmic-ray interaction model in which median, minimal and maximal proton fluxes are used are taken from Mori[28]. Solid curve: $F_{\rm CR}$ (median p-flux) + $F_{\rm pulsar}$; short-dashed curve: $F_{\rm CR}$ (maximal p-flux) + $F_{\rm pulsar}$; long-dashed curve: F_{CR} (minimal p-flux) + $F_{\rm pulsar}$; dotted curve: F_{CR} (median p-flux); dot-dashed curve: $F_{\rm pulsar}$.

In fig. 3, we show the comparisons of the model predictions with the observed data, where $\dot{N}_{\rm NS100} f_\gamma = 1$ has been used. The χ^2 test for comparing the model result (solid curve) with the observed data gives 2.5 per degree of freedom for 29 observed data when $c1 = 0.94$. We believe that such χ^2 value should be acceptable. In fig. 3, we also show the model results in which the maximal (short-dashed curve) and minimal (long-dashed curve) proton spectra given by Mori (1997) are used respectively. It can be seen that the observed data except for one in the energy range from 30 GeV to 50 GeV are within model predictions. It can be seen that the unresolved pulsars contribute very little to the diffuse Galactic γ-ray emission at lower energies but they significantly contribute to the diffuse emission above 1 GeV. For example, the unresolved pulsars can account for ~50% of the observed intensity above 1 GeV for $\dot{N}_{\rm NS100} f_\gamma = 1$ in our model[29]. We have also applied this method to calculate the duffuse γ-rays from LMC and SMC and found that the diffuse γ-ray flux is also dominated by the contribution of pulsars for $E_\gamma > 1$ GeV[30].

4 Conclusions

We have used our pulsar model to study the statistical properties of the γ/X-ray pulsars. Our results indicate that our model can successfully explain the X-ray and γ-ray emission from spinpowered pulsars. It should be pointed out that some improvements are needed although some successes of our model have been obtained, for example the details of pulsar magnetosphere and phase emission characteristics of γ-ray pulsars[31].

Acknowledgements This work was partially supported by RGC grant of Hong Kong Government and Natural Science Foundation of Yunnan Province.

References

1. Harding, A. K., Pulsar gamma-*rays*-spectra, luminosities, and efficiencies, ApJ, 1981, 245: 267.
2. Dermer, C. D., Sturner, S. J., On the energetics and number of gamma-ray pulsars, ApJ, 1994, 420: L75.
3. Cheng, K. S., Ho, C., Ruderman, M. A., Energetic radiation from rapidly spinning (I)——outer magnetosphere gaps, ApJ, 1986a, 300: 500.
4. Cheng, K. S., Ho, C., Ruderman, M. A., Energetic radiation from rapidly spinning (II)——Vela and Crab, ApJ, 1986b, 300: 522.
5. Ho, C., Spectra of crab-like pulsars, ApJ, 1989, 342: 369.
6. Chiang, J., Romani, R. W., Gamma radiation from pulsar magnetospheric gaps, ApJ, 1992, 400: 629.
7. Cheng, K. S., Ding, W. K. Y., Pulsed gamma-ray emission from short-period pulsars, ApJ, 1994, 431: 724.
8. Cheng, K. S., Wei, D. M., The synchrotron self-Compton model for X-ray and gamma-ray emission from pulsars, ApJ, 1995, 448: 281.
9. Romani, R. W., Gamma-ray pulsars: radiation processes in the outer magnetosphere, ApJ, 1996, 470: 469.
10. Zhang, L., Cheng, K. S., High-energy radiation from rapidly spinning pulsars with thick outer gaps, ApJ, 1997, 487: 370.
11. Bailes, M., Kniffen, D. A., Galactic gamma-ray from radio pulars, ApJ, 1992, 391: 659.
12. Yadigaroglu, I. A., Romani, R. W., Gamma-ray pulsars: beaming evolution, statistics, and unidentified EGRET sources, ApJ, 1995, 449: 211.
13. Sturner, S. J., Dermer, C. D., Statistical analysis of gamma-ray properties of rotation-powered pulsars, ApJ, 1996, 461: 872.
14. Cheng, K. S., Gil, J., Zhang, L., Nonthermal origin of X-rays from rotation-powered neutron stars, ApJ, 1998, 493: L35.
15. Cheng, K. S., Zhang, L., Multicomponent X-ray emissions from regions near or on the pulsar surface, ApJ, 1999, 515: 337.
16. Becker, W., Trümper, J., The X-ray luminosity of rotation-powered neutron stars, A&A, 1997, 326: 682.
17. Cheng, K. S., Zhang, J. L., General radiation formulae for a relativistic charged particle moving in curved magnetic field lines: the synchrocurvature radiation mechanism, ApJ, 1996, 463: 271.
18. Cheng, K. S., Zhang, L.,The statistics of gamma-ray pulsars, ApJ, 1998, 498: 327.
19. Nel, H. I. et al., EGRET high-energy gamma-ray pulsar studies (III)—a survey, ApJ, 1996, 465: 898.
20. Zhang, L., Cheng, K. S., The gamma-ray conversion efficiency of rotation-powered pulsars, MNRAS, 1998a, 294: 177.
21. Zhang, L., Cheng, K. S., Which unidentified EGRET sources are gamma-ray pulsars? A&A, 1998b, 335: 234.
22. Paczynski, B., A test of the galactic origin of gamma-ray bursts, ApJ, 1990, 348: 485.
23. Emmering, R. T., Chevalier, R. A., The intrinsic luminosity and inital period of pulsars, ApJ, 1989, 345: 931.
24. Lyne, A. G., Manchester, R. N., The shape of pulsar radio beams, MNRAS, 1988, 234: 477.
25. Biggs, J. D., Meridional compression of radio pulsar beams, MNRAS, 1990, 245: 514.
26. Hunter, S. D. EGRET observations of the diffuse gamma-ray emission from the galactic plane, ApJ, 1997, 381: 205.
27. Pohl, M., Kanbach, G., Hunter, S. D. et al., The pulsar contribution to the diffuse galactic gamma-ray emission, ApJ, 1997, 491: 159.
28. Mori, M., The galactic diffuse gamma-ray spectrum from cosmic-ray proton interactions, ApJ, 1997, 478: 225.
29. Zhang, L., Cheng, K. S., The galactic diffuse gamma-ray spectrum from unresolved rotation-powered pulsars, MNRAS, 1998c, 301: 841.
30. Zhang, L., Cheng, K. S., The contribution of pulsars to diffuse gamma-rays in the Large Magellanic cloud, MNRAS, 1998d, 294: 729.
31. Cheng, K. S., Ruderman, M., Zhang, L., A three dimensional outer-mangetospheric gap model for gamma-ray pulsars: geometry, pair production, emission morphologies and phase-resolved spectra, ApJ, 1999.